Research Article | Vol. 12, No. 6 / 1 June 2021 / Biomedical Optics Express 3485
Biomedical Optics EXPRESS

Light scattering in intraocular lenses explanted 15 to 40 years after surgery

JORGE L. ALIO,[1,2] AUGUSTO ARIAS,[3] FRANCESCO D'ORIA,[1,2,4] FRANCESCA TOTO,[1,2] JORGE ALIO DEL BARRIO,[1,2] RAUL DUARTE,[3] AND PABLO ARTAL[3,*]

[1]*Vissum innovation, Alicante, Spain*
[2]*Division of Ophthalmology, Universidad Miguel Hernández, Alicante, Spain*
[3]*Laboratorio de Óptica, Universidad de Murcia, Campus de Espinardo (Edificio 34), Murcia 30100, Spain*
[4]*Section of Ophthalmology, Department of Basic Medical Science, Neuroscience and Sense Organs, University of Bari, Bari, Italy*
[*]*Corresponding author: pablo@um.es*

Abstract: The optical quality of intraocular lenses (IOLs) of different materials that have been implanted from 16 to 44 years in human eyes was studied. The IOLs were explanted due to other causes than loss of transparency. The scattered light from the IOLs was assessed in two angular regimes by using dark field images (for wide angles) and the optical integration method (for narrower angles). No evident differences were found in the scattering intensities processed from the dark images. The explanted lenses presented slightly increased amounts of straylight between 1 and 5.1° when compared to a reference new unused lens.

1. Introduction

Straylight in pseudophakia has been studied during the last decades [1,2]. A recent literature review shows that in the absence of posterior capsule opacification (PCO), straylight is increased to a level that can lead to severe functional difficulties in 10% of pseudophakic eyes [3]. This could be attributed to postoperative complications related to the implanted intraocular lens (IOL). A main concern is biocompatibility of IOL materials: once implanted in the human eye, the material of the lenses starts interacting with the intraocular environment of the anterior segment and the long-term results of such interaction are ignored. Also, the IOL may suffer in the very long term a degradation caused by the ageing of the material itself. Indeed, during cataract surgery with IOL implantation, the blood-aqueous barrier is disrupted, with proteins and cells released in the aqueous humor. Proteins then adsorb on the IOL surface and influence subsequent cellular reactions on the IOL [4]. It has been suggested that blood cells, devitalized cells, bacterial, inflammatory cells or lipids may provide an initial nidus for calcification [5]. Over the time, several clinical and material degradations of implanted IOLs have been reported, including photochemical material alterations, internal and surface calcific deposits, water vacuolation (glistenings) and discoloration [6]. The clinical significance of all these degradations is variable, with some resulting in minimal optical impairment and others in significant visual disturbance and the need for IOL explantation. A multicenter retrospective study performed in 2012 to analyze all data from cases of IOL explantation, concluded that IOL opacification was the third most common reason for IOL explantation [7].

The optical degradation of the IOLs has already been studied in explanted lenses by analyzing the loss of transparency [6]. However, there is a lack of published evidence investigating the effects of long term IOL material optical degradation and the possible loss of optical quality. IOLs explanted due to other causes than loss of transparency are an excellent opportunity to study optical ageing of the IOL's materials. Such study seems to be today relevant, especially

#423652 https://doi.org/10.1364/BOE.423652
Journal © 2021 Received 1 Mar 2021; revised 28 Apr 2021; accepted 13 May 2021; published 18 May 2021

Biomedical Optics EXPRESS

because in the recent years the age of patients being the subject of cataract surgery has decreased and consequently the anticipated duration of the IOLs in the eye has significantly increased [8].

The aim of this study is to investigate for the first time the change in optical quality through the analysis of the scatter in two angular regimes from IOLs of different materials implanted from 16 to 44 years in phakic and pseudophakic human eyes.

2. Material and methods

We performed an ex-vivo study on 8 IOLs of different materials, phakic and pseudophakic, that have been previously implanted for 16 to 44 years in human eyes and have been explanted due to dislocation or development of cataract or corneal endothelial decompensation. Scattering was assessed in two angular regimes: at wide angles (around 30°) by recording dark field images and at narrower angles (lower than 5.1°) by implementing the optical integration method [9].

2.1. Surgical technique

In cases of foldable pseudophakic IOLs, the lenses were removed in one piece through scleral incisions performed at the steep corneal meridian, to avoid astigmatism induction. After filling the anterior chamber with a dispersive viscoelastic (VISCOAT OVD, Alcon, USA), the IOL was dissected from the capsular bag using a cohesive viscoelastic (ProVisc OVD, Alcon, USA) with a 30G cannula. Using a Sinskey hook and a Lester hook (Katena, USA), the IOL was loosened from the capsular bag; afterwards, the IOL was passed through the scleral incision to complete the explantation. The explantation was performed trying to minimize any damage to the lenses' optics. In case of intra-operative damage, or in case it was necessary to partially bisect the IOLs for the explantation with coaxial forceps, such lenses were excluded from the present study. In the case of unfoldable phakic PMMA IOL, the whole lens was removed through a sclera or corneal wound without cutting the lens [7]. The IOLs, once explanted, were stored in a balanced salt solution at room temperature.

2.2. Explanted lenses

Eight IOLs of 4 different materials explanted from 8 patients were studied. The mean patient age at the time of IOL explantation was 54 ± 14 years (range 41 to 70 years). Table 1 represents the characteristics of the studied IOLs, including IOL model and manufacturer, optic material composition, reason for explantation and time interval between implantation and explantation.

The explanted IOL models were: Acrysof MA60MA (Alcon), GBR (IOLTECH), ICM120V4 (STAAR Visian ICL), ZB5M (Baikoff), ZSAL-4 (Morcher GMBH) and Artisan aphakia (Ophtec); in 1 case of angle-supported phakic IOL was not possible to define the exact model of the lens. None of the lenses analyzed in this paper were explanted due to opacification or showed any signs of opacification at the pre-operative slit-lamp examination. The mean interval between the initial surgery and the IOL explantation was 24 ± 9 years. A new, non-implanted, monofocal IOL (Tecnis ZCB00; Abott Medical Optics Inc., The Netherlands) was also measured for comparison purposes.

2.3. Optical analysis

2.3.1. Dark field photography

Dark field pictures of the IOLs were recorded to evaluate their located opacities. Figure 1 shows the schematic diagram of the custom-built apparatus for the acquisition of the dark field images where the light from a ring of white LEDs is scattered in the IOL. The ring is inside a black box with a small window such that only the scattered light is imaged and acquired by a CMOS camera. The parameters of the camera (i.e., gain and exposure time) were fixed for the acquisition of all tested IOLs, allowing a direct comparison among them. The scattered light in the optical zone

Biomedical Optics EXPRESS

Table 1. Characteristics of the studied intraocular lenses.[a]

Patient Number	IOL Model	Manufacturer	Optic Material Composition	Reason for Explantation	Time Interval (years)
364	Acrysof MA60MA	Alcon, Inc.	Acrylic hydrophobic	IOL dislocation	24
453	GBR	IOLTECH	Silicon	Endothelial failure with corneal edema	16
379	Acrysof MA60MA (?)	Alcon, Inc.	Acrylic hydrophobic	IOL dislocation	44
1474	Unknown AS-PIOL	Unknown	PMMA	Endothelial failure with corneal edema	>20
293	ICM120V4	STAAR Visian ICL	Collamer	Cataract	20
452	ZB5M	Baikoff	PMMA	Cataract	28
460	ZSAL-4	Morcher GMBH	PMMA	Cataract	21
1469	Artisan aphakia	Ophtec	PMMA	Cataract	>20

[a]Abbreviation: AS-PIOL, Angle-supported Phakic Intraocular Lenses; PMMA, Polymethyl methacrylate

of the IOL was assessed by the mean of the scattered intensities (MSI). MSI was calculated as the mean of the gray levels within a disk with 3 mm of diameter around the IOL center. The saturated pixels (i.e., with gray values of 255) were excluded for this calculation.

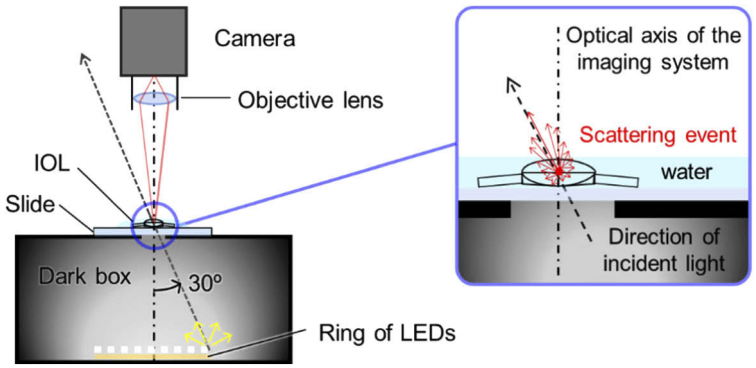

Fig. 1. Setup for the dark field photography. Only the scattered light is captured by the camera.

2.3.2. Optical integration method

The angular dependence of the straylight (s) of the IOLs is quantified as the product between the point spread function (PSF) and the angle squared (θ):

$$s(\theta) = \theta^2 PSF(\theta) \tag{1}$$

The PSF, as function of θ, was measured by using the optical integration method [9]. This is based on the projection of disks, with uniform irradiance and diameter of 2θ, through the IOL while the central intensity ($Ic(\theta)$) of their images is recorded. Ic corresponds to the summation of

Biomedical Optics EXPRESS

the weighted contributions PSF(φ) from all the bright sources at a radial distance φ within the disk. Mathematically:

$$I_c(\theta) = \int_0^{\theta} 2\pi\varphi PSF(\varphi)d\varphi \tag{2}$$

After normalizing $Ic(\theta)$ to its maximum value, $PSF(\theta)$ is calculated as:

$$PSF(\theta) = \frac{1}{2\pi\theta}\frac{dIc(\theta)}{d\theta} \tag{3}$$

Figure 2 shows the instrument for the implementation of the optical integration method. The disks were generated with a Digital Light Processing (DLP) projector (LightCrafter Display 4710 EVM; Texas Instruments Inc., USA). The entrance pupil of the system consists of the collimating L1 lens and the circular aperture AP. A telescope composed of the L2 and L3 lenses conjugates the entrance pupil with the IOL which is immersed in a wet cell with physiological saline (0.9% NaCl). The diameter of the illumination on the IOL is 4 mm. A spectral filter (FB550-40; Thorlabs Inc., Germany) was placed between L2 and L3 lenses to produce quasi-monochromatic illumination on the IOL. The central wavelength and bandwidth of the illumination were 550.4 and 42 nm, respectively. In the case of IOLs with positive power, the disks were directly imaged on a CMOS camera (DCC1545M; Thorlabs Inc., Germany) by the L4 and L5 lenses. For IOLs with negative powers, the focusing was recovered by incorporating the L6 lens (LB1811-A; Thorlabs Inc., Germany). The camera was axially displaced to adjust the focus for each IOL. Additionally, the amount of straylight provided by the optical system (or the baseline) was measured when the wet cell was without IOL and the L6 lens in place.

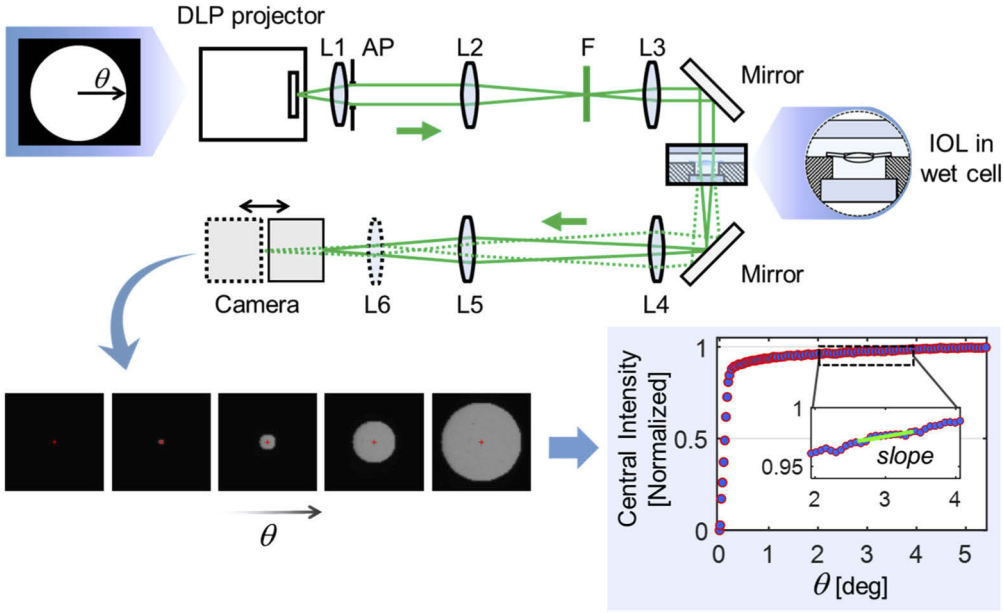

Fig. 2. Instrument for the assessment of the straylight as function of θ for the tested IOLs. Solid ray tracing depicts the light trajectory when IOLs with positive power are tested. In the case of negative IOLs, the light is focused in the camera by incorporating the L6 lens in a conjugated plane with the IOL, as represented by the dashed tracing. The focusing for each IOL is manually adjusted by the axial displacement of the camera.

Initially, for the calculation of the straylight, several disks with sizes of 2θ are displayed by the projector and the central intensity on their images (on the position marked by the red cross) is

Biomedical Optics EXPRESS

recorded. The angular distribution of the PSF is calculate from the angular local slopes of the central intensity, according to Eq. (3). F is a spectral filter. AP is a circular aperture.

For each straylight measurement, the processed central intensity corresponds to the mean of three sequential measurements. 114 disks were displayed to complete a set of central intensity measurements. The dark noise of the camera and the effects of parasitic light were compensated by subtracting the intensity – at the center of the projected disks – for a zero matrix displayed on the projector to the recorded central intensities. We found a proper angular sampling by using two increments of θ: 0.024 and 0.070° for angles lower and higher than 1.1°, respectively. Figure 2 shows examples of the acquired disks and the central intensity as function of θ. The local angular slopes of the central intensity were computed to calculate the PSF following Eq. (3). The slopes were estimated by linear fitting the central intensity with the angle within a range of ±0.4° around θ. The angular range of PSF is 5.1°. It is mainly determined by the size of the DLP matrix and the focal length of L1 lens. The PSFs retrieved with Eq. (3) are normalized on the solid angle of 25.9×10^{-3} steradian (sr). The units of PSF and s are sr^{-1} and $deg^2 sr^{-1}$.

The area under $s(\theta)$ was calculated between 1 and 5.1° (the domain of scattered light) to facilitate the analysis of the measurements. By considering the discrete data, it was compute as:

$$Area\ under\ s(\theta) = \sum_{n=Ni}^{Nf} (\theta_i - \theta_{i-1}) \frac{s(\theta_i) + s(\theta_{i-1})}{2} \tag{4}$$

where the Ni and Nf are the numbers of the θ vector for which $\theta(Ni)$ and $\theta(Nf)$ are equals – or closest – to 1 and 5.1°, respectively. The units of this area are $deg^3 sr^{-1}$.

3. Results

Figure 3(a) shows the dark field images of the tested IOLs. Although the new lens (non-implanted) Tecnis ZCB00 IOL was clear, its dark field picture is affected by some parasitic reflections and remaining dirt on the supporting slide. On the other hand, opacifications distributed over the optical area of the IOLs with reference 460, 364 and 379 were identified. Localized opacifications (i.e., white spots) were observed in the 293, 379 and 1474 IOLs that were probably originated in their manipulation during the extraction. Figure 3(b) shows the forward scattered light quantified by the MSI values in the IOLs and the supporting slide. The MSI values as function of the time since the implantation of the IOLs (with this available data in Table 1) are depicted in Fig. 3(c). The coefficient of determination of a linear fitting between the two variables was poor (R^2=0.06), suggesting lack of correlation between them.

The angular dependence of the straylight in the tested positive and negative IOLs are respectively shown in Figs. 4(a) and 4(b). In some angular ranges, the straylight amounts of Tecnis and IOLs numbered as 1474 and 460 are slightly lower than the baseline, demonstrating the clearness of those IOLs. The amount of straylight generated by IOLs numbered as 452, 1469 and 364 is higher than the corresponding amount for an elderly healthy eye (according to the Commission Internationale de l'Eclairage, CIE) in different angular ranges. Figure 4(c) shows the area under each measured angular profile of straylight. The difference among those areas and the corresponding one for the baseline, as function of the time since the implantation of the IOLs, is plotted in Fig. 4(d). In general, the amount of straylight increases as the time increases. However, there is not a clear relationship between those quantities.

Biomedical Optics EXPRESS

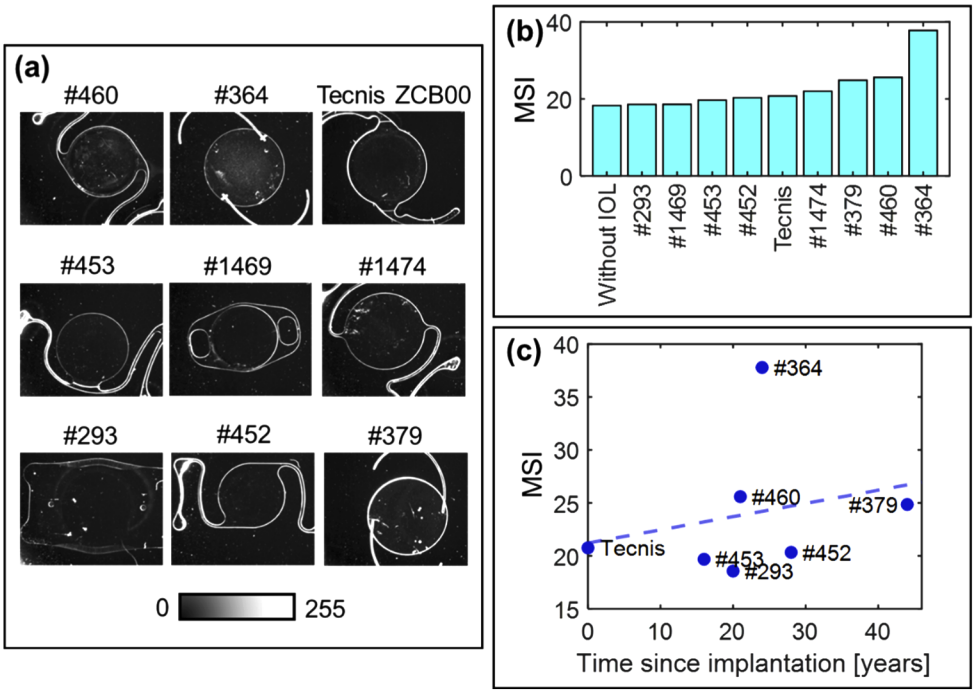

Fig. 3. Acquired and quantified scattering from dark field photography. (a) Dark field images. (b) Mean of the scattered intensities (MSI) within the optical area of IOLs and supporting slide (without IOL). (c) MSI values as function of the time since implantation for IOLs with this information available (see Table 1). The dashed blue line depicts the linear fitting (R^2=0.06).

Biomedical Optics EXPRESS

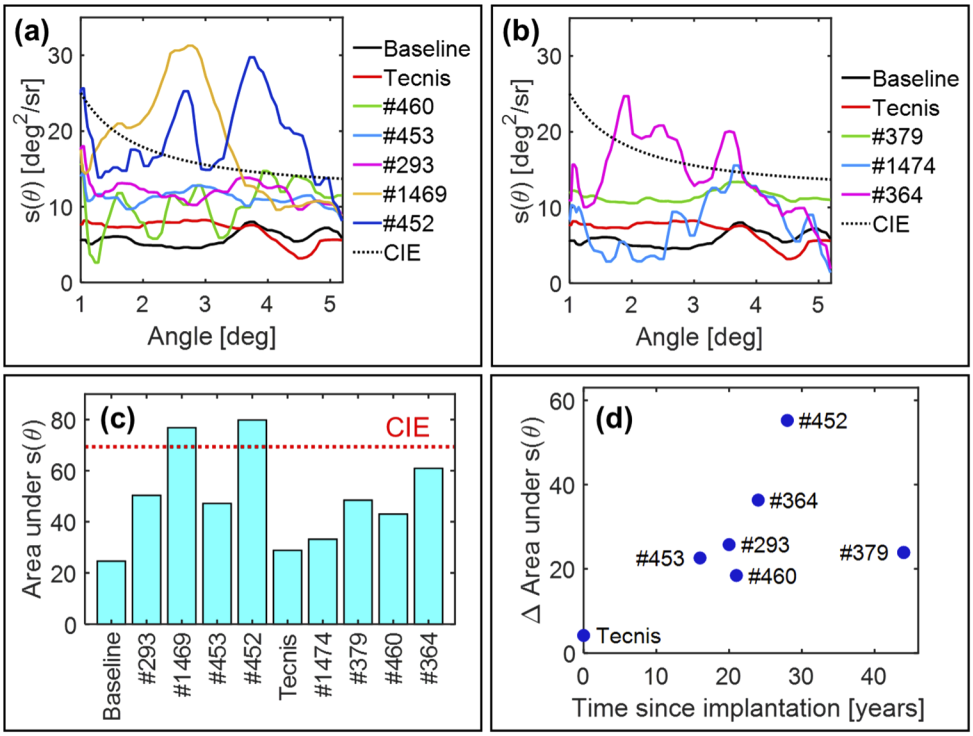

Fig. 4. Straylight in tested IOLs. Angular distribution of the (a) positive and (b) negative IOLs, the non-implanted Tecnis IOL, a biconvex lens (i.e., baseline) and an elderly (70 y.o.) eye according to the CIE standards. (c) Area under the straylight profiles, preserving the order from Fig. 3(b). (d) Areas, referred to the corresponding baseline value, as function of the time since implantation of the IOLs with this available data. The units of the area under the s(θ) profile are deg^3/sr.

4. Discussion

We quantified the scattered light, within two angular regimes, in IOLs with time intervals of implantation between 16 and 44 years. The straylight at wide angles (approximately 30°) was captured by dark field photography. For angles between 1 and 5.1°, the straylight parameter (s) was measured and compared with the expected value for an elderly and healthy eye, according to the CIE. The light is deviated to each angular range depending to the size of the scatterers. For instance, according to the diffraction angle, spatial variations of the refractive index or surface profile with periods longer than 6.2 μm are associated to the light contributions at narrow angles. Because of the small number of tested IOLs, no correlation was found between the amount of light scattered at a wide angle and the time interval of the implantation (see Fig. 3(c)). On the other hand, we found that the total amount of straylight between 1 and 5.1° increases as the time interval of implantation increases in most of the tested IOLs (see Fig. 4(d)). However, we found only a small difference in the amounts of straylight provided by long-term implanted IOLs compared to an estimated healthy elderly eye, according to the CIE reports (Fig. 4(c), dotted red line). This supports the hypothesis that it is necessary to have those lenses implanted in the eye for a longer time to experience those changes in a clinically relevant level.

The straylight in the pseudophakic eye is on average 2-fold higher than that in a young healthy eye (i.e., 20 years old), according to a retrospective analysis with 1533 eyes involved [3]. Our results follow those findings in the tested IOLs. The mean area under the straylight profiles

Biomedical Optics EXPRESS

between 1 and 5.1° (see Fig. 4(a) and (b)) for the explanted IOLs is 55.0 deg^3/sr that approximately corresponds to the double of this amount for the baseline (24.6 deg^3/sr). The straylight levels of the latter at 3.5° (6.5 deg^2/sr) are similar to that in a young eye (~8.9 deg^2/sr [10]). A study [11] on 74 pseudophakic IOLs explanted from donor eyes found a mean straylight value of 5.8 deg^2/sr ±4.7 (SD) at 2.5°. The implantation times were not specified in this study. In our results, this mean was 10.3 deg^2/sr ±7.9 (SD) at the same angle. The difference could be due to a different range of implantation times, being longer in the IOLs tested here.

Large straylight levels found in some pseudophakic patients are commonly attributed to opacifications of the IOL [3,12,13].

Glistening are liquid-filled microvacuoles accumulated within the lens polymer over time [14–19]. Due to the different refractive index between the glistenings and the IOL material, they act as refractive particles that glisten at slit lamp examination. This is mostly reported in IOLs made of a hydrophobic acrylic material [19]. In our investigation, glistenings were not visible in any of the lenses at pre-operative slit-lamp examination. However, IOL # 364, made of hydrophobic acrylic, seems affected by glistening, presents the highest MSI values from its dark field image (see Fig. 3(b)). The other IOL of hydrophobic acrylic (#379), that was implanted for a longer time, presents lower straylight amounts in both angular regimes. Calcifications can be produced by the material, with most prevalence in hydrophilic acrylic lenses and a pre-existing environmental circumstances [5]. Optical quality analysis of the explanted opacified IOLs showed significant reduction of modulation transfer function values, suggesting that patients may experience a reduction of resolution [20]. However, IOL calcification is not likely to cause increased straylight without being other clinically diagnosed: none of the studied lenses showed signs of opacification on the preoperative slit-lamp examination, thus discarding the opacification as a cause of increased straylight in the studied IOLs. Snowflake degeneration is associated to the slowly progressive PMMA degradation by the ultra-violet light exposure [21,22]. The IOL #1474, made of PMMA, could be affected by this degradation. However, its MSI value (see Fig. 3(b)) is moderate and its mean amount of straylight between 1 and 5.1° is the lowest among the group of explanted IOLs.

Straylight peaks in IOLs #1469 (at 2.7°) and # 452 (at 3.8°), observed in Fig. 4(a) and (b), would related to spatial periods of 12 and 8 microns, respectively, in the refractive index and/or the surface profile. Generally, the variations on the height of the IOL surfaces are corrected by the polishing. As some of the tested IOLs were manufactured long-time ago, it is necessary to take into account that quality control in this industry has changed over time with an expected positive impact on the optical quality. Therefore, apart from the interaction between the IOL and the ocular media, another contributing factor to the generation of straylight is the roughness of the IOL. However, in this work, those features were not investigated.

The number of tested IOLs in this study is too small to conclude what influence the material has on the scattering generation or to establish a general relationship between amount of straylight and implantation time. In spite of this, the measurements shown here can be useful for a further understanding of phenomena associated to light scattering of long-time implanted eye using for instance the double-pass technique or optical integration [23,24].

5. Conclusions

This investigation is the first study of scattering performed on lenses explanted due to other causes than loss of transparency after 16 to 44 implant years. It is the first work that tries to study the optical decay suffered by these lenses inside the eye. Both phakic and pseudophakic lenses were included. The results indicate a modest deterioration of the optical quality of IOLs through time that might be very important for the future development of intraocular lenses. Wide-angle scatter was very similar in the explanted lenses and in new ones. Narrow-angle scatter increased with the time implanted but without reaching the level of older eyes according

Biomedical Optics EXPRESS

to CIE. Further investigations on this topic are needed to support these outcomes, studying how long-term implanted phakic and pseudophakic lenses suffer for optical deterioration and differences between both groups and different types of materials.

Funding. Agencia Estatal de Investigación (PID2019-105684RB-I00AEI10.13039/501100011033); Instituto de Salud Carlos III; Fundación Séneca (19897/GERM/15).

Acknowledgements. We would like to thank Rodriguez AE and Mena Guevara KJ for their cooperation in the experimental methods of this investigation.

Disclosures. The authors declare no conflicts of interest

Data availability. Data underlying the results presented in this paper are not publicly available at this time but may be obtained from the authors upon reasonable request.

References

1. G. L. Van der Heijde, J. Weber, and R. Boukes, "Effects of straylight on visual acuity in pseudophakia," Doc. Ophthalmol. **59**(1), 81–84 (1985).
2. F. K. Witmer, H. J. B. den Brom, A. C. Kooijman, and L. J. Blanksma, "Intra-ocular light scatter in pseudophakia," Doc. Ophthalmol. **72**(3-4), 335–340 (1989).
3. G. Łabuz, N. J. Reus, and T. J. T. P. van den Berg, "Ocular straylight in the normal pseudophakic eye," J. Cataract Refractive Surg. **41**(7), 1406–1415 (2015).
4. L. Werner, "Biocompatibility of intraocular lens materials," Curr. Opin. Ophthalmol. **19**(1), 41–49 (2008).
5. I. M. Neuhann, G. Kleinmann, and D. J. Apple, "A new classification of calcification of intraocular lenses," Ophthalmol. **115**(1), 73–79 (2008).
6. N. Stanojcic, C. Hull, and D. P. O'Brart, "Clinical and material degradations of intraocular lenses: A review," Eur. J. Ophthalmol. **30**(5), 823–839 (2020).
7. R. Fernandez-Buenaga and J. L. Alio, "Intraocular Lens Explantation After Cataract Surgery: Indications, Results, and Explantation Techniques," Asia-Pac. J. Ophthalmol. **6**(4), 372–380 (2017).
8. J. C. Erie, K. H. Baratz, D. O. Hodge, C. D. Schleck, and J. P. Burke, "Incidence of cataract surgery from 1980 through 2004: 25-year population-based study," J. Cataract Refractive Surg. **33**(7), 1273–1277 (2007).
9. H. Ginis, G. M. Pérez, J. M. Bueno, and P. Artal, "The wide-angle point spread function of the human eye reconstructed by a new optical method," J. Vis. **12**(3), 20 (2012).
10. J. J. Vos, B. L. Cole, H. W. Bodmann, E. Colombo, T. Takeuchi, and T. J. T P. Van Den Berg, CIE Equations for Disability Glare, 2002
11. G. Łabuz, N. J. Reus, and T. J. T. P. van den Berg, "Light scattering levels from intraocular lenses extracted from donor eyes," J. Cataract Refractive Surg. **43**(9), 1207–1212 (2017).
12. R. Lapid-Gortzak, I. J. E. van der Meulen, J. W. van der Linden, M. P. Mourits, and T. J. T. P. van den Berg, "Straylight before and after phacoemulsification in eyes with preoperative corrected distance visual acuity better than 0.1 logMAR," J. Cataract Refractive Surg. **40**(5), 748–755 (2014).
13. J. J. Rozema, T. Coeckelbergh, M. Caals, M. Bila, and M. J. Tassignon, "Retinal straylight before and after implantation of the bag in the lens IOL," Invest. Ophthalmol. Visual Sci. **54**(1), 396–401 (2013).
14. E. Mönestam and A. Behndig, "Impact on visual function from light scattering and glistenings in intraocular lenses, a long-term study," Acta. Ophthalmol. **89**(8), 724–728 (2011).
15. J. Colin, D. Praud, D. Touboul, and C. Schweitzer, "Incidence of glistening with the latest generation of yellow-tinted hydrophobic acrylic intraocular lenses," J. Cataract Refractive Surg. **38**(7), 1140–1146 (2012).
16. A. Chang, A. Behndig, M. Rønbeck, and M. Kugelberg, "Comparison of posterior capsule opacification and glistenings with 2 hydrophobic acrylic intraocular lenses: 5- to 7-year follow-up," J. Cataract Refractive Surg. **39**(5), 694–698 (2013).
17. D. K. Dhaliwal, N. Mamalis, R. J. Olson, A. S. Crandall, P. Zimmerman, O. C. Alldredge, F. J. Durcan, and O. Omar, "Visual significance of glistenings seen in the AcrySof intraocular lens," J. Cataract Refractive Surg. **22**(4), 452–457 (1996).
18. U. Gunenc, F. H. Oner, S. Tongal, and M. Ferliel, "Effects on visual function of glistenings and folding marks in AcrySof intraocular lenses," J. Cataract Refractive Surg. **27**(10), 1611–1614 (2001).
19. C. Schweitzer, I. Orignac, D. Praud, O. Chatoux, and J. Colin, "Glistening in glaucomatous eyes: visual performances and risk factors," Acta. Ophthalmol. **92**(6), 529–534 (2014).
20. T. Tandogan, R. Khoramnia, C. Y. Choi, A. Scheuerle, M. Wenzel, and P. Hugger, "Optical and material analysis of opacified hydrophilic intraocular lenses after explantation: a laboratory study," BMC Ophthalmol. **15**(1), 170 (2015).
21. D. J. Apple, Q. Peng, S. N. Arthur, L. Werner, J. H. Merritt, L. G. Vargas, D. S. Hoddinott, M. Escobar-Gomez, and J. M. Schmidbauer, "Snowflake degeneration of polymethyl methacrylate posterior chamber intraocular lens optic material: a newly described clinical condition caused by unexpected late opacification of polymethyl methacrylate," Ophthalmology **109**(9), 1666–1675 (2002).
22. L. Werner, J. C. Stover, J. Schwiegerling, and K. K. Das, "Effects of intraocular lens opacification on light scatter, stray light, and overall optical quality/performance," Invest. Ophthalmol. Visual Sci. **57**(7), 3239–3247 (2016).

Biomedical Optics EXPRESS

23. J. Santamaría, P. Artal, and J. Bescós, "Determination of the point-spread function of human eyes using a hybrid optical–digital method," J. Opt. Soc. Am. A **4**(6), 1109–1114 (1987).
24. A. Arias, H. Ginis, and P. Artal, "Straylight in Different Types of Intraocular Lenses," Trans. Vis. Sci. Tech. **9**(12), 16 (2020).